analytical chemistry

LETTER

pubs.acs.org/ac

Virus−Poly(3,4-ethylenedioxythiophene) Composite Films for Impedance-Based Biosensing

Keith C. Donavan,[†] Jessica A. Arter,[†] Rosa Pilolli,[‡] Nicola Cioffi,[‡] Gregory A. Weiss,*[,†] and Reginald M. Penner*[,†]

[†]Department of Chemistry, University of California, Irvine, California 92697-2025, United States

[‡]Dipartimento di Chimica, Università degli Studi di Bari Aldo Moro, Bari, Italy I-70126

ABSTRACT: Composite films composed of poly(3,4-ethylenedioxythiophene), PEDOT, and the filamentous virus M13-K07 were prepared by electrooxidation of 3,4-ethylenedioxythiophene (EDOT) in aqueous solutions containing 8 nM of the virus at planar gold electrodes. These films were characterized using atomic force microscopy and scanning electron microscopy. The electrochemical impedance of virus−PEDOT films increases upon exposure to an antibody (p-Ab) that selectively binds to the M13 coat peptide. Exposure to p-Ab causes a shift in both real (Z_{RE}) and imaginary (Z_{IM}) impedance components across a broad range of frequencies from 50 Hz to 10 kHz. Within a narrower frequency range from 250 Hz to 5 kHz, the increase of the total impedance (Z_{total}) with p-Ab concentration conforms to a Langmuir adsorption isotherm over the concentration range from from 6 to 66 nM, yielding a value for K_d = 16.9 nM at 1000 Hz.

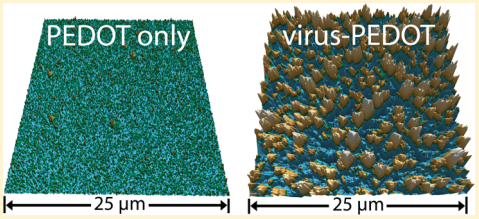

The use of whole virus particles as a bioaffinity matrix to recognize and bind target analytes is a concept that was first demonstrated in 2003 by Petrenko and Vodyanoy.[1] Subsequent work from this group provided the proof-of-concept for the use of bioaffinity matrixes composed of whole virus particles.[2−4] From these early studies, an active subfield of phage-mediated biosensing is rapidly emerging (for recent reviews, see refs 5 and 6). Previously, we have investigated electrochemical biosensors in which a covalently attached layer of the filamentous phage, M13, is employed as the bioaffinity matrix on a planar gold electrode.[7−9] In these devices, the virus layer is attached to the gold surface via a self-assembled thiolate monolayer.[9] The binding of analyte to the virus layer is detected using electrochemical impedance spectroscopy as an increase in the impedance of the surface at high frequencies, above 4 kHz.[7−9] The detection of analyte molecules in these studies has been both label-free and "direct", in the sense that redox reporter species have not been added to the system,[10] but a modest limit-of-detection (LOD) of 20 nM has been obtained for an antibody to the P8 major coat protein of the M13 virion.[7] This LOD is imposed by a maximum resistance change at these covalent virus layers of just 10 Ω.[7,8] We have postulated that this resistance change is limited by the total thickness of the virus layer responsible for generating the impedance signal; this thickness approximately equals the length of a filamentous virus particle of 1.0 μm in the case of M13. To increase this resistance change and to extend the LOD to lower values, we have sought methods for creating thicker, three-dimensional, porous matrixes in which virus particles are embedded.

An interesting candidate transducer material consists of an electronically conductive organic polymer into which virus particles have been entrained during the polymerization process. We have recently shown[11] that nanowires composed of a composite of an electronically conductive polymer, poly(3,4-ethylenedioxythiophene) or PEDOT, and M13 can be prepared by electrodeposition. Here, we have prepared layers of this same virus−PEDOT composite on planar gold electrodes and used electrochemical impedance spectroscopy to transduce the binding of an antibody to the virus particles entrained within this layer. Initial work on the incorporation of virus particles into conducting polymers was demonstrated by Ionescu et al.,[12] where T7 phage were used to display a peptide from the West Nile virus which was then tested against the West Nile virus antibody. In that study, the virus−polymer film composite was prepared using a two step synthetic procedure involving the adsorption of the monomer and biomolecules onto the electrode surface first, followed by electropolymerization.[12] Antibody was detected using a sandwich assay scheme involving a secondary peroxidase-labeled antibody that generated H_2O_2 for electrochemical detection. In this Letter, the synthesis of PEDOT−virus composite layers is described and we demonstrate that an antibody for M13 can be detected with an LOD of 6 nM in a label-free, direct fashion using electrochemical impedance spectra (EIS). An attractive aspect of this approach is that a fully functional bioaffinity layer is produced, beginning with a metal electrode, in a single electrochemical step requiring a few minutes. In contrast, the preparation of bioaffinity layers consisting of covalently linked antibodies or virus particles on electrode surfaces, as in our prior work, typically involves 3−5 chemical steps and more than one day. The last of these steps, required to thwart nonspecific binding to the bioaffinity layer, involves passivation of

Received: January 11, 2011
Accepted: February 28, 2011
Published: March 09, 2011

Scheme 1. Polymerization of (a) EDOT and (b) EDOT with M13 Virus Incorporation

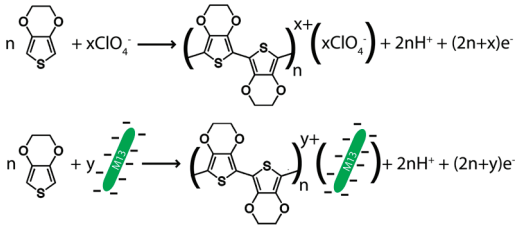

the surface by exposure to solutions of bovine serum albumin (BSA), casein, or other globular proteins. As reported below, we find that this blocking step is unnecessary for virus−PEDOT films, at least for the antibodies we have attempted to detect here. Intrinsically, the PEDOT film surface has a low affinity for a nonbinding antibody.

The virus−PEDOT composite was synthesized by electrooxidation from 3,4 ethylenedioxythiophene (EDOT)[13] in the presence of 8 nM M13, as previously described.[11] One significant advantage of PEDOT is its biocompatibility,[14] and the creation of biocompatible layers has motivated the synthesis of PEDOT−biomolecule composite films.[14−16] In particular, the work of Asplund et al.[16] showed that large, negatively charged biomolecules including fibrinogen, hyaluronic acid, and heparin could be used as counterion dopants for the polymerization of EDOT to form a tightly bound composite film. Here, we extend this strategy, shown in Scheme 1, to an even larger biological object, the M13 virus particle.

EXPERIMENTAL SECTION

Materials. All chemicals and reagents were purchased from Sigma-Aldrich and used as received, unless otherwise noted. Anti-M13 antibody (p-Ab, GE Healthcare Life Sciences) and anti-FLAG antibody (n-Ab, Sigma) were used as received. Milli-Q UV water was used as the solvent for all solutions. Phosphate buffered fluoride (PBF, 4.2 mM Na_2HPO_4, 1.5 mM KH_2PO_4 and 140 mM NaF) was pH adjusted to 7.2 and vacuum filtered through a 0.22 μm filter (Corning). The run buffer employed for all EIS measurements contained 0.1% Tween-20 (Acros) in PBF buffer.

Synthesis of Phage−PEDOT Films. Circular gold electrodes (3 mm diameter, CH Instruments) were manually polished with diamond polishing pastes with particles sizes of 1, 0.25, and 0.1 μm (Ted Pella) on a polishing microcloth (Buehler) and sonicated in nanopure water for 10 min each. The electrodes were then cleaned in piranha solution (3:1 H_2SO_4/H_2O_2) for 10 min, rinsed with water, and dried under a stream of purified nitrogen. A flame-cleaned platinum wire counter electrode was wrapped around the polymer barrel of the polished gold electrode, as previously described.[7,9] These electrodes were then placed in the phage−PEDOT plating solution (12.5 mM $LiClO_4$, 2 mM EDOT, and 8 nM M13 bacteriophage) and allowed to equilibrate for 1 min. Electropolymerization occurred by cycling between 0.2 and 0.8 V vs mercurous sulfate electrode (MSE) for 10 cycles using a PARSTAT 2273 controlled with POWERCV software (Princeton Applied Research, Oak Ridge, TN) at a scan rate of 50 mV/s. Synthesized films were rinsed in Milli-Q water three times and immediately transferred into the run buffer.

Electrochemical Impedance Spectroscopy. Freshly synthesized phage−PEDOT films were equilibrated in run buffer for 10 min, and then five consecutive EIS were acquired using a PARSTAT 2273 potentiostat controlled by POWERSine software (Princeton Applied Research, Oak Ridge, TN). A 10 mV voltage modulation amplitude was used in these measurements, and 50 frequency data points were acquired spanning 0.1 Hz to 1 MHz at 0.0 V vs MSE. The electrode was then washed 3 times each with run buffer, PBF buffer, and water before being exposed to n-Ab. The phage−PEDOT film was incubated in solutions of n-Ab in PBF for 30 min followed by rinsing with run buffer, PBF, and water, before the electrode was placed back into the run buffer and allowed to equilibrate for 10 min. Five EIS were then acquired; the electrode was rinsed with run buffer, PBF, and water, and this process was repeated with PBF solutions containing p-Ab.

AFM and SEM Analysis and Film Thickness Measurements. AC Mode atomic force microscopy (AFM) imaging was performed on PEDOT films both with and without phage in ambient conditions using an Asylum MFP-3D-SA atomic force microscope (Asylum Research, Santa Barbara, CA) in conjunction with Olympus AC160TS AFM tips (Olympus). Topographs were obtained over a 25 μm range at 512 × 512 pixels. These images were line-by-line flattened using the Asylum image processing software. Scanning electron microscopy (SEM) was performed on uncoated films using a Philips XL30 FEG SEM at an operating voltage of 10.0 keV. The PEDOT−virus film thickness was measured by electrodepositing these films on photolithographically patterned gold-coated glass microscope slides. This process involved spin-coating photoresist (Shipley 1808, MicroChem) on the surface of gold-coated slides, photopatterning the resist with 10 μm lines, and developing the photoresist to produce alternating 10 μm-wide strips of bare gold and photoresist. The electrodeposition of PEDOT−virus films was then carried out according to the procedure described above; the films were rinsed with water, and the photoresist was removed with acetone to expose a clean, gold-coated surface enabling a direct measurement of the film thickness using AFM.

RESULTS AND DISCUSSION

Composite virus−PEDOT films were prepared by cycling the potential of a 3 mm diameter gold electrode in aqueous 12.5 mM $LiClO_4$, 2.0 mM EDOT, and 8 nM M13 at 50 mV/s (Figure 1a). The EDOT oxidation current increased monotonically with each scan, indicating an increasing electrode area consistent with growth of an electronically conductive virus−PEDOT film. To assess the growth rate of this composite film, films were electrodeposited onto lithographically patterned gold electrodes on glass enabling accurate AFM film thickness measurements to be carried out. The virus−PEDOT film increased linearly in thickness by 0.13 μm/scan (Figure 1b).

The morphology of the phage−PEDOT and PEDOT-only films prepared using ten deposition scans were examined using both SEM and AFM (Figure 2c−f). Images of PEDOT-only films, prepared under identical conditions to virus−PEDOT films except for the absence of virus in the plating solution, showed smooth, featureless surfaces (Figure 2c,e) as previously reported.[17] The rms roughness of these surfaces measured by AFM was ≈20 nm. When 8 nM of M13 phage was added to the deposition solution, an increase in the roughness of the film surface was observed (Figure 2d). SEM images of these

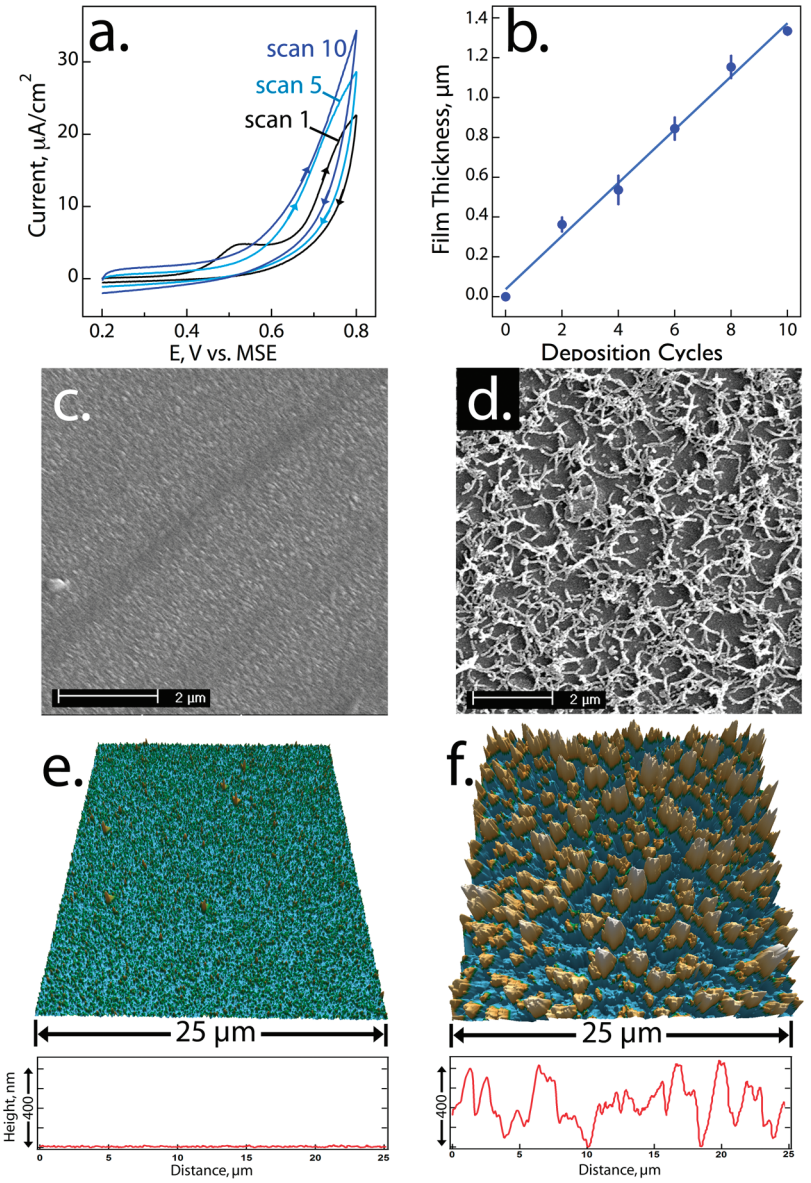

Figure 1. Electrodeposition of a virus−PEDOT composite film on gold. (a) Cyclic voltammograms at 50 mV/s in aqueous 12.5 mM $LiClO_4$, 2.0 mM EDOT, and 8 nM M13 bacteriophage. The films studied in Figure 2 were prepared using ten deposition cycles on a 3 mm diameter gold electrode. (b) Plot of virus−PEDOT film thickness, measured on photolithographically patterned films using AFM, as a function of the number of deposition cycles. (c,d) SEM images showing the topography of a PEDOT film (c) and a virus−PEDOT−film (d). Both films were prepared using ten deposition cycles. (e,f) AFM images of a PEDOT film (e) and a virus−PEDOT composite film (f), both prepared using ten deposition cycles. (f). A representative line scan from each of these AFM images is shown at bottom. The rms roughness of the two films was ≈10 nm and ≈400 nm, respectively.

virus−PEDOT films show a high areal density of filaments with an apparent diameter of ≈100 nm emerging from a planar background (Figure 2d,f). Since the diameter of a single M13 virus particle is 6 nm, these filaments must consist of bundles including 10−20 virus particles. In prior work involving the preparation of composition protein−PEDOT films,[16] SEM images qualitatively similar to the images reported here have been obtained. In AFM images, these filaments extend 100−400 nm above the base of the film leading to a rms roughness of ≈400 nm (Figure 2f).

Electrochemical impedance spectra (EIS) of phage−PEDOT films were acquired for freshly synthesized virus−PEDOT films (and PEDOT-only control films) after exposure to three aqueous solutions: (1) in PBF run buffer, (2) after a 30 min incubation with the noninteracting anti-FLAG antibody (n-Ab), and (3) after incubation with the anti-M13 antibody (p-Ab). After 30 min exposures to either n-Ab or p-Ab, the electrode was rinsed and transferred to PBF run buffer for impedance analysis to ensure that the solution resistance was constantly maintained. A Nyquist plot for one virus−PEDOT electrode (Figure 2a) shows the high frequency regime below 10 kHz for the three solutions. Impedance values observed after exposure to 66 nM n-Ab (red) closely approximate those seen in the PBF run buffer (black) at each frequency, but a clear shift to higher Z_{RE} and Z_{IM} is apparent after exposure to 66 nM p-Ab (green) across the entire frequency range. Empirically, we found that the total impedance, Z_{total}, provided higher sensitivity than either Z_{RE} or Z_{IM} for the detection of p-Ab by the composite virus−PEDOT films. On

dx.doi.org/10.1021/ac2000835 |*Anal. Chem.* 2011, 83, 2420–2424

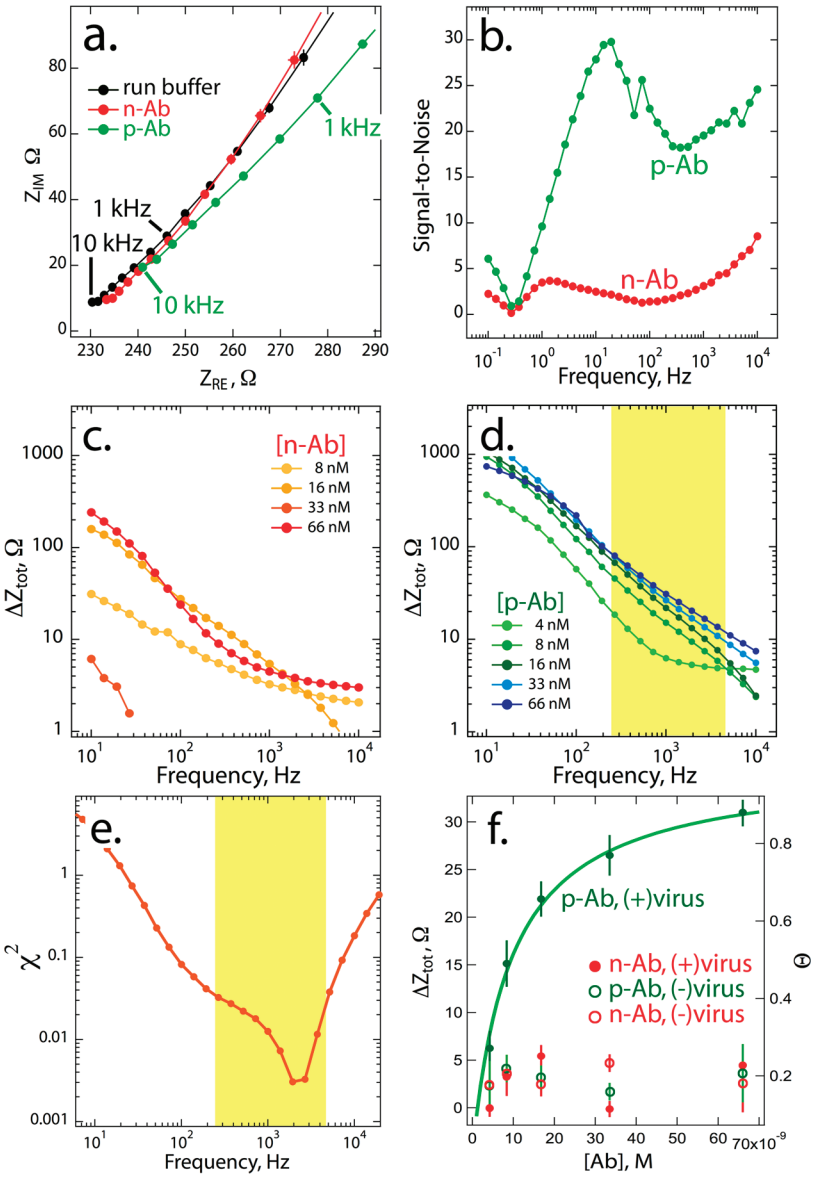

Figure 2. (a) Nyquist plots for a phage−PEDOT film (thickness ≈ 1.2 μm) immersed in PBF buffer (black) and PBF buffer + [p-Ab] = 66 nM (green) and PBF buffer + [n-Ab] = 66 nM (red). Five impedance measurements in each solution were averaged to obtain each curve; error bars, obscured by the data points in some cases, indicate $\pm 1\sigma$. (b) Plot of the signal-to-noise ratio, defined as $\Delta Z_{tot}/\sigma$, versus frequency. [p-Ab] = [n-Ab] = 66 nM. (c,d) Log−log plots of ΔZ_{tot} versus frequency for a series of p-Ab (c) and n-Ab (d) concentrations ranging from 4 nM to 66 nM. In (d), the yellow interval indicates frequencies where ΔZ_{tot} increases monotonically with [p-Ab]. (e). χ^2 versus frequency for the fit of a Langmuir isotherm to the ΔZ_{tot} versus [p-Ab] data shown in (d). The minimum of this plot, corresponding to the best fit, is observed at 2 to 3 kHz. (f) Plot of ΔZ_{total} versus concentration for a PEDOT film containing M13, labeled (+) virus, and a second film containing no virus, labeled (−) virus. These two films were exposed to both n-Ab and p-Ab at the indicated concentrations. Impedance data for p-Ab exposures at the virus−PEDOT composite film are fitted with a Langmuir isotherm.

the basis of this analysis, we use the total impedance measured versus the PBF run buffer, ΔZ_{total}, as the sensor "signal".

The frequency-dependent signal-to-noise (S/N) of p-Ab detection (Figure 2b) in the 66 nM loading solution was obtained by dividing ΔZ_{total} by the standard deviation of five consecutive impedance measurements. Defined in this way, the S/N for p-Ab increases sharply with increasing frequency above 1 Hz, reaching a maximum of 28 at 10 Hz ranging from 20 to 25 at frequencies up to 10 kHz whereas the detection of n-Ab, also at 66 nM, produced lower S/N values from 4 (1 Hz) to 8 (10 kHz).

The ability of the virus−PEDOT film to detect p-Ab and discriminate against n-Ab was assessed by measuring the concentration dependence of the ΔZ_{total} from 10 Hz to 10 kHz (Figure 2c,d). A comparison of Figure 2c with Figure 2d shows that ΔZ_{total} is approximately an order of magnitude larger for p-Ab versus n-Ab across this entire frequency range, but a closer examination of the concentration dependence for p-Ab from 4 nM to 66 nM (Figure 2d) reveals that ΔZ_{total} increases monotonically with [p-Ab] for frequencies between 250 Hz and 5 kHz, highlighted in yellow in Figure 2d. Outside of this frequency range, ΔZ_{total} does not track [p-Ab] and the virus−PEDOT electrode does not function properly as a detector for p-Ab.

A more quantitative assessment of the correlation between [p-Ab] and ΔZ_{total} as a function of frequency is possible if we

dx.doi.org/10.1021/ac2000835 |*Anal. Chem.* 2011, 83, 2420–2424

hypothesize a functional form for this relationship. A Langmuir isotherm can be used to model our data as it is frequently used to interpret biosensor response functions:

$$K_d = \frac{1-\theta}{\theta} \quad (1)$$

where θ is the fraction of available binding sites on the surface occupied by p-Ab. We must further make an assumption about the relationship between θ, ΔZ_{total}, and $\Delta Z_{total,max}$, the maximum total impedance shift observed at $\theta = 1.0$. We can assume, as in the prior work of Huang et al.,[18] that a linear relationship exists between these quantities:

$$\Delta Z_{total} = \theta \Delta Z_{total,max} \quad (2)$$

The conformance of our experimental [p-Ab] versus ΔZ_{total} data to eqs 1 and 2 can be evaluated by plotting the goodness-of-fit parameter, χ^2, versus frequency (Figure 2e). We see that a minimum in χ^2 is obtained in the center of the yellow frequency band, near 3 kHz. If we choose a frequency in the vicinity of this minimum (1 kHz in Figure 2f), we observe that the experimental ΔZ_{total} versus [p-Ab] plot is well represented by a Langmuir isotherm (Figure 2f). In this specific example, the K_d derived from the fit yields a value of 16.9 nM, slightly higher than the $K_d \approx 0.5$ nM we have obtained previously[8] using quartz crystal microbalance gravimetry. These data afford an estimated minimum LOD of ≈6 nM for p-Ab.

What causes the impedance increase observed upon p-Ab binding to the entrained phage particles in our PEDOT films? Our data does not permit this mechanism to be specified with certainty, but our working hypothesis is that a combination of the displacement of ionically conductive buffer solution and pore-blocking by p-Ab likely increases the ionic resistance of the composite film, elevating Z_{RE}. This mechanism has been invoked to account for the increased Z_{RE} seen upon p-Ab binding to covalently tethered virus layers on gold electrode surfaces.[7,9] Alternatively, in other biosensor systems, it has been proposed that analyte binding induces a decrease in the dielectric constant of the capture layer, resulting in a decrease in capacitance and an increase in Z_{IM},[19] similar to what we have reported here for virus−PEDOT films.

CONCLUSIONS

Copolymerization with EDOT provides a simple method for rapidly and reproducibly immobilizing virus particles on electrode surfaces. A fully functional bioaffinity layer, consisting of a virus−PEDOT composite film, is thereby fabricated in a single electrochemical operation requiring a few minutes. When the impedance of this composite layer was monitored, the specific binding of an antibody was observed with a limit-of-detection of ≈6 nM. This LOD is made possible by the fact that the PEDOT−virus layer intrinsically limits nonspecific binding of antibody, even absent is the use of blocking layers of BSA, casein, etc. that are typically required. These results provide motivation for the optimization of the composite film, especially concerning the virus loading, the film thickness, film geometry, and the growth program employed for film deposition. Given that virus particles can be programmed to recognize and bind a wide range of biomolecules,[5] our hope is that the scheme demonstrated here can serve as the basis for a general biosensing strategy.

AUTHOR INFORMATION

Corresponding Author
*E-mail: rmpenner@uci.edu (R.M.P.).

ACKNOWLEDGMENT

R.M.P. acknowledges the financial support of this work from the National Science Foundation (CHE-0956524), and G.A.W. acknowledges support from the NAID (1 R43 AI074163) and the NCI (R01 CA133592-01) of the National Institutes of Health.

REFERENCES

(1) Petrenko, V.; Vodyanoy, V. *J. Microbiol. Methods* **2003**, *53*, 253–262.
(2) Nanduri, V.; Balasubramanian, S.; Sista, S.; Vodyanoy, V. J.; Simonian, A. L. *Anal. Chim. Acta* **2007**, *589*, 166–172.
(3) Nanduri, V.; Sorokulova, I. B.; Samoylov, A. M.; Simonian, A. L.; Petrenko, V. A.; Vodyanoy, V. *Biosens. Bioelectron.* **2007**, *22*, 986–992.
(4) Olsen, E.; Sorokulova, I.; Petrenko, V.; Chen, I.; Barbaree, J.; Vodyanoy, V. *Biosens. Bioelectron.* **2006**, *21*, 1434–1442.
(5) Weiss, G. A.; Penner, R. M. *Anal. Chem.* **2008**, *80*, 3082–3089.
(6) Mao, C.; Liu, A.; Cao, B. *Angew. Chem., Int. Ed.* **2009**, *48*, 6790–6810.
(7) Yang, L.-M. C.; Diaz, J. E.; McIntire, T. M.; Weiss, G. A.; Penner, R. M. *Anal. Chem.* **2008**, *80*, 5695–5705.
(8) Yang, L.-M. C.; Diaz, J. E.; McIntire, T. M.; Weiss, G. A.; Penner, R. M. *Anal. Chem.* **2008**, *80*, 933–943.
(9) Yang, L.; Tam, P.; Murray, B.; McIntire, T.; Overstreet, C.; Weiss, G.; Penner, R. *Anal. Chem.* **2006**, *78*, 3265–3270.
(10) Hvastkovs, E. G.; Buttry, D. A. *Analyst* **2010**, *135*, 1817–1829.
(11) Arter, J.; Taggart, D.; McIntire, T.; Penner, R.; Weiss, G. *Nano Lett.* **2010**, *10*, 4858–4862.
(12) Ionescu, R. E.; Cosnier, S.; Herrmann, S.; Marks, R. S. *Anal. Chem.* **2007**, *79*, 8662–8668.
(13) Luo, S.-C.; Ali, E. M.; Tansil, N. C.; Yu, H.-H.; Gao, S.; Kantchev, E. A. B.; Ying, J. Y. *Langmuir* **2008**, *24*, 8071–8077.
(14) Richardson-Burns, S. M.; Hendricks, J. L.; Foster, B.; Povlich, L. K.; Kim, D.-H.; Martin, D. C. *Biomaterials* **2007**, *28*, 1539–1552.
(15) Asplund, M.; Thaning, E.; Lundberg, J.; Sandberg-Nordqvist, A. C.; Kostyszyn, B.; Inganas, O.; von Holst, H. *Biomed. Mater.* **2009**, *4*, 045009.
(16) Asplund, M.; von Holst, H.; Inganas, O. *Biointerphases* **2008**, *3*, 83–93.
(17) Wang, X.; Sjoberg-Eerola, P.; Eriksson, J.-E.; Bobacka, J.; Bergelin, M. *Synth. Met.* **2010**, *160*, 1373–1381.
(18) Huang, Y.; Bell, M. C.; Suni, I. I. *Anal. Chem.* **2008**, *80*, 9157–9161.
(19) Daniels, J. S.; Pourmand, N. *Electroanalysis* **2007**, *19*, 1239–1257.